ALIEN EARTHS

Which Nearby Planetary Systems Are Likely to Host Habitable Planets and Life?

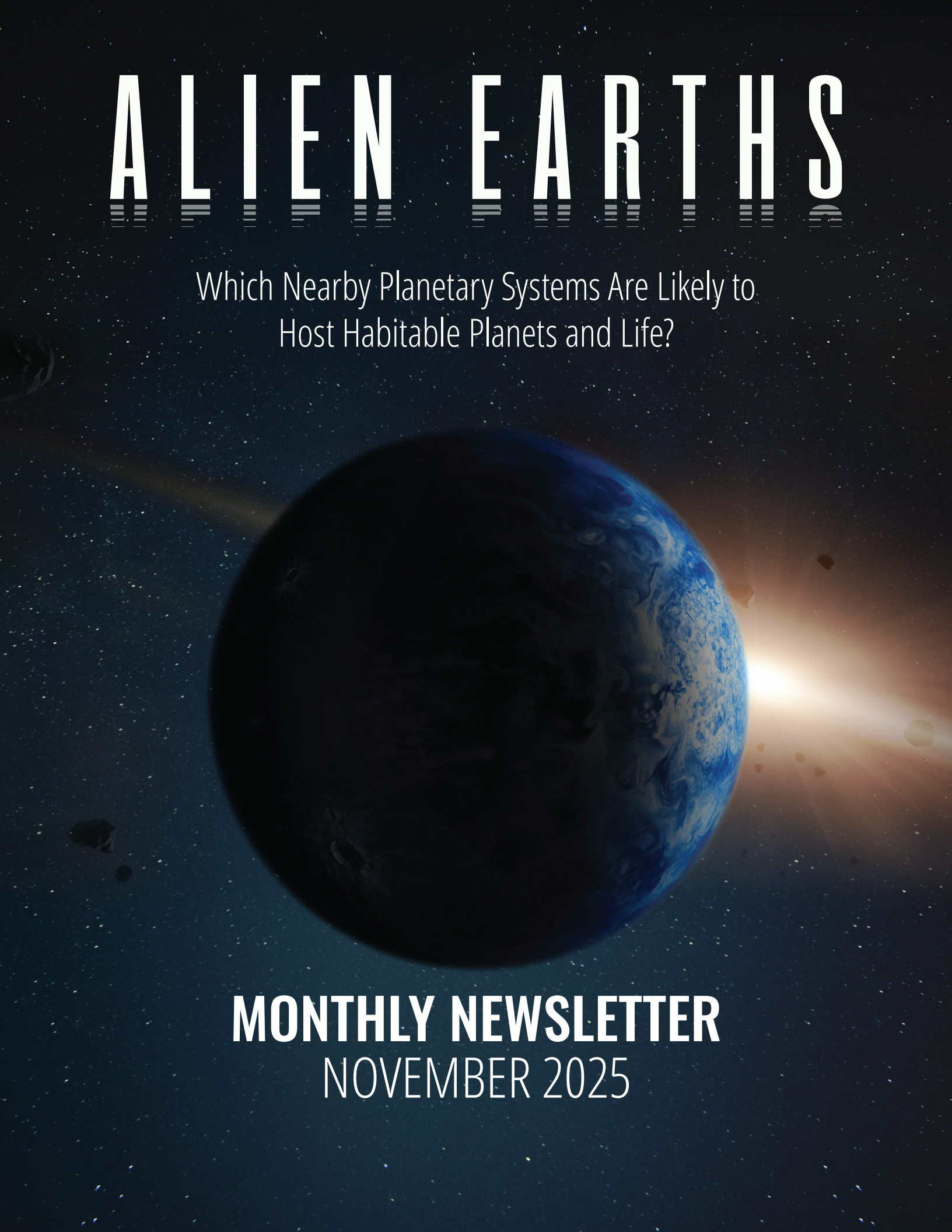

MONTHLY NEWSLETTER

NOVEMBER 2025

Alien Earths is part of NASA's Nexus for Exoplanetary System Science program, which carries out coordinated research toward the goal of searching for and determining the frequency of habitable extrasolar planets with atmospheric biosignatures in the Solar neighborhood.

Our interdisciplinary teams includes astrophysicists, planetary scientists, cosmochemists, material scientists, chemists, biologists, and physicists.

The Principal Investigator of Alien Earths is Daniel Apai (University of Arizona). The projects' lead institutions are The University of Arizona's Steward Observatory and Lunar and Planetary Laboratory.

For a complete list of publications, please visit the AE Library on the SAO/NASA Astrophysics Data System.

Alien Earths All-Hands Meeting 2026

You are invited to attend the **Alien Earths All Hands Meeting**, taking place **February 3-6, 2026** at the **Hacienda del Sol** in Tucson! The meeting will kick off at noon on Tuesday, February 3 and continue through Friday, February 6, wrapping up after lunch. Join us for a week of science highlights, group discussions, and collaboration across the Alien Earths team.

We can't wait to see everyone there!

For questions or link to registration, please contact rstratton@arizona.edu.

Recent Publications

Dynamical Masses for 23 Pre-Main Sequence Stars in Upper Scorpius: A Critical Test of Stellar Evolutionary Models

……

Analytical estimates for heliocentric escape of satellite ejecta

……

Testing the performance of cross-correlation techniques to search for molecular features in JWST NIRSpec G395H observations of transiting exoplanets

……

ExoMiner++: Enhanced Transit Classification and a New Vetting Catalog for 2-minute TESS Data

……

HWO Target Stars and Systems: A Prioritized Community List of Potential Stellar Targets for the Habitable Worlds Observatory's ExoEarth Survey

……

Diversity in Planetary Architectures from Pebble Accretion: Water Delivery to the Habitable Zone with Pebble Snow

……

Gravity-sensitive Spectral Indices in Ultracool Dwarfs: Investigating Correlations with Metallicity and Planet Occurrence Using SpeX and Fire Observations

……

PLATOSpec's first results: Planets WASP-35b and TOI-622b are on aligned orbits, and K2-237b is on a polar orbit

Dynamical Masses for 23 Pre-Main Sequence Stars in Upper Scorpius: A Critical Test of Stellar Evolutionary Models

Towner, A. P. M. ; Eisner, J. A. ; Sheehan, P. D. ; Hillenbrand, L. A. ; Wu, Y. -L.

eprint arXiv:2509.23001

We present dynamical masses for 23 pre-main sequence K- and M-type stars in the Upper Scorpius star-forming region. These masses were derived from the Keplerian rotation of CO disk gas using the MCMC radiative-transfer package pdspy and a flared-disk model with 15 free parameters. We compare our dynamical masses to those derived from five pre-main sequence evolutionary models, and find that most models consistently underestimate stellar mass by ≳25%. Models with updated treatment of stellar magnetic fields are a notable exception − they consistently return stellar masses in good agreement with the dynamical results. We find that the magnetic models' performance is valid even at low masses, in contrast with some literature results suggesting they may overestimate stellar mass for M⋆ ≲ 0.6 M⊙. Our results are consistent with dynamical versus isochronal evaluations for younger samples (e.g. Taurus, 1-3 Myr), and extend the systematic evaluation of stellar evolutionary models up to stars ∼11 Myr in age. Finally, we derive disk dust masses to evaluate whether using dynamical masses versus isochronal masses changes the slope of the log(Mdust)−log(M⋆) relation. We derive a slightly shallower relation using dynamical masses versus isochronal masses, but the slopes of these relations agree within uncertainties. In all cases, we derive a steeper-than-linear relation for log(Mdust)−log(M⋆), consistent with previous literature results for Upper Sco.

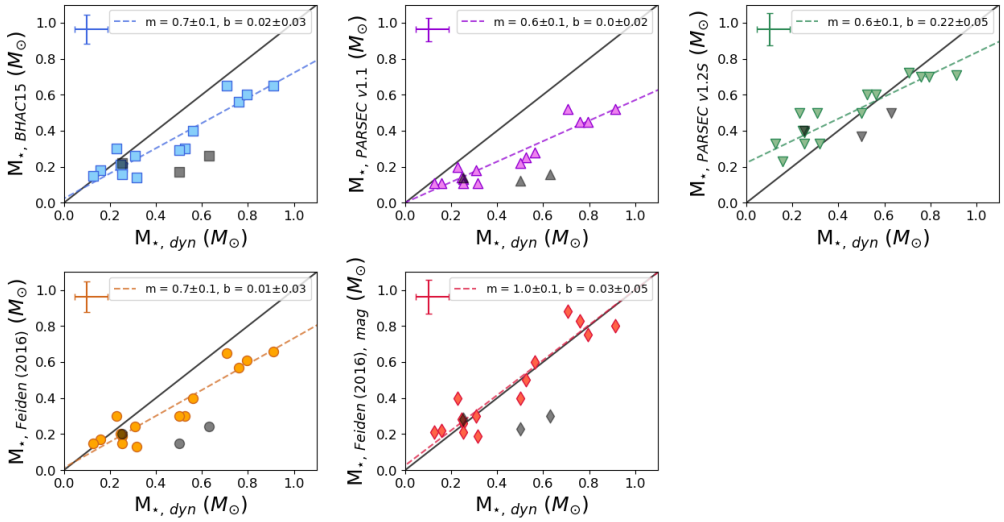

***Figure 8**. Comparison of stellar masses returned by each PMS evolutionary model set to the dynamical masses we derive using pdspy. The color scheme is the same as in Figure 7. In all panels, the isochronal mass is shown on the y-axis, and the dynamical mass (same in all cases) is shown on the x-axis. The black dotted line represents a 1:1 relation in all panels. The ODR best-fit line slope (m) and intercept (b) are listed in each panel. Top row: BHAC15 (left), PARSEC v1.1 (Bressan et al. 2012) (center), PARSEC v1.2S (Chen et al. 2014) (right). Bottom row: non-magnetic models of Feiden (2016) (left), magnetic models of Feiden (2016) (center). The significant improvement in agreement of the magnetic models of Feiden (2016) with the dynamical masses, as compared to the other PMS evolutionary models tested here, can be clearly seen in the bottom center panel. A figure covering the full range of masses can be found in Appendix C.*

Analytical estimates for heliocentric escape of satellite ejecta

Castro-Cisneros, Jose Daniel; Malhotra, Renu; Rosengren, Aaron J.

Icarus, Volume 445, id.116845

We present a general analytic framework to assess whether impact ejecta launched from the surface of a satellite can escape the gravitational influence of the planet–satellite system and enter heliocentric orbit. Using a patched-conic approach and defining the transition to planetocentric space via the Hill sphere or sphere of influence, we derive thresholds for escape in terms of the satellite-to-planet mass ratio and the ratio of the satellite's orbital speed to its escape speed. We identify three dynamical regimes for ejecta based on residual speed and launch direction. We complement this analysis with the circular restricted three-body problem, deriving a necessary escape condition from the Jacobi integral at L2 and showing that it is consistent with the patched–conic thresholds. Applying our model to the Earth–Moon system reveals that all three outcomes — bound, conditional, and unbound — are accessible within a narrow range of launch speeds. This behavior is not found in other planetary satellite systems, but may occur in some binary asteroids. The framework also shows that the Moon's tidal migration has not altered its propensity to produce escaping ejecta, reinforcing the plausibility of a lunar origin for some near-Earth asteroids.

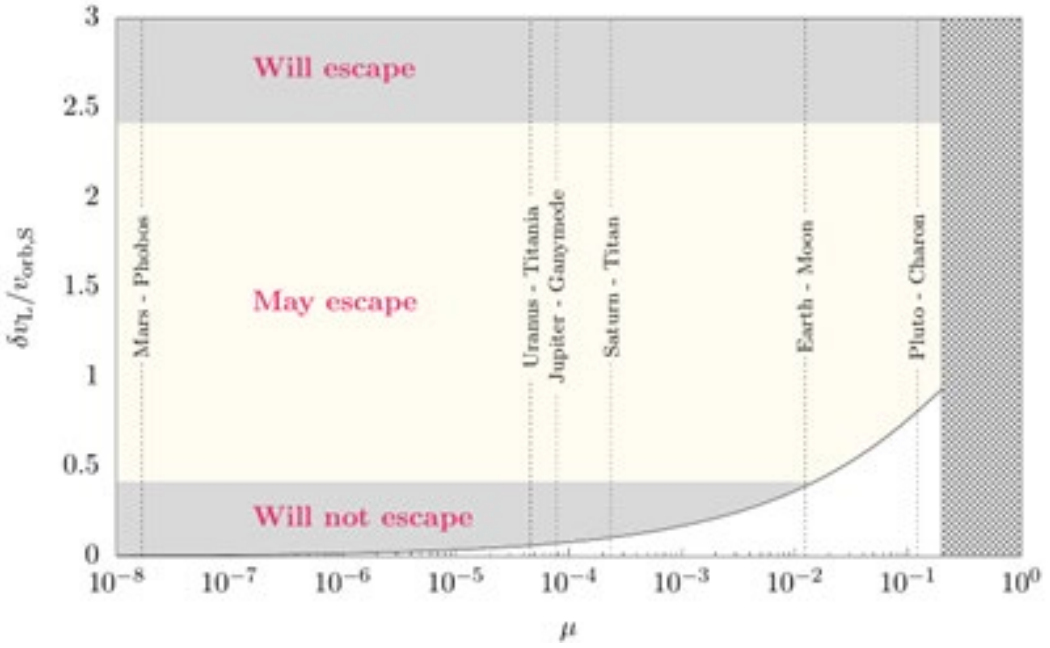

Figure 2. Ratio of residual speed at the satellite's Hill sphere and the satellite orbital speed, versus the satellite-to-planet mass ratio μ. The curve shows the bounding case of particles launched with speed equal to the satellite's escape velocity. *Shaded* regions represent the regions of different outcomes for ejecta launched above escape velocity. The *stippled* region is the range of $\mu > 0.2$ where the patched-conics approximation becomes less effective.

Testing the performance of cross-correlation techniques to search for molecular features in JWST NIRSpec G395H observations of transiting exoplanets

Esparza-Borges, Emma; López-Morales, Mercedes ; Pallé, Enric ; Makhnev, Vladimir ; Gordon, Iouli; Hargreaves, Robert ; Kirk, James; Cáceres, Claudio ; Crossfield, Ian J. M. ; Crouzet, Nicolas; Decin, Leen ; Désert, Jean-Michel ; Flagg, Laura ; Muñoz, Antonio García ; Harrington, Joseph ; Molaverdikhani, Karan; Morello, Giuseppe ; Nikolov, Nikolay; Solmaz, Arif; Rackham, Benjamin V.; Redfield, Seth

Monthly Notices of the Royal Astronomical Society, Volume 543, Issue 4, pp. 3456-3473, 18 pp.

Cross-correlations techniques offer an alternative method to search for molecular species in James Webb Space Telescope (JWST) observations of exoplanet atmospheres. In a previous article, we applied cross-correlation functions for the first time to JWST NIRSpec/G395H observations of exoplanet atmospheres, resulting in a detection of CO in the transmission spectrum of WASP-39b and a tentative detection of CO isotopologues. Here, we present an improved version of our cross-correlation technique and an investigation into how efficient the technique is when searching for other molecules in JWST NIRSpec/G395H data. Our search results in the detection of more molecules via cross-correlations in the atmosphere of WASP-39b, including H2O and CO2, and confirms the CO detection. This result proves that cross-correlations are a robust and computationally cheap alternative method to search for molecular species in transmission spectra observed with JWST. We also searched for other molecules (CH4, NH3, SO2, N2O, H2S, PH3, O3, and C2H2) that were not detected, for which we provide the definition of their cross-correlation baselines for future searches of those molecules in other targets. We find that that the cross-correlation search of each molecule is more efficient over limited wavelength regions of the spectrum, where the signal for that molecule dominates over other molecules, than over broad wavelength ranges. In general, we also find that Gaussian normalization is the most efficient normalization mode for the generation of the molecular templates.

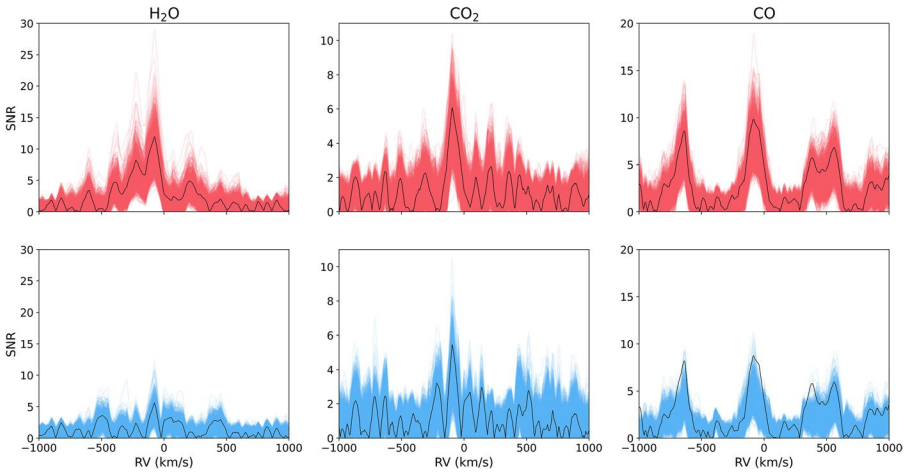

Figure 7. *Results of the cross-correlation search of (left panels), (middle panels), and (right panels) along their optimal wavelength ranges over the 2000 samples of the transmission spectrum (those shown in Figs 4, 5, and 6). Black-solid lines show the CCFs resulting from the cross-correlation search over the original transmission spectrum. Top panels show the results using the Gaussian normalization mode and bottom panels show the results using the frequency filter normalization mode.*

ExoMiner++: Enhanced Transit Classification and a New Vetting Catalog for 2-minute TESS Data

Valizadegan, Hamed; Martinho, Miguel J. S.; Jenkins, Jon M.; Twicken, Joseph D.; Caldwell, Douglas A.; Maynard, Patrick; Wei, Hongbo; Zhong, William; Yates, Charles; Donald, Sam; Collins, Karen A.; Latham, David; Barkaoui, Khalid; Calkins, Michael L.; Carden, Kylee; Chazov, Nikita; Esquerdo, Gilbert A.; Guillot, Tristan; Krushinsky, Vadim; Nowak, Grzegorz; Rackham, Benjamin V.; Triaud, Amaury; Schwarz, Richard P.; Stephens, Denise; Stockdale, Chris; Watkins, Cristilyn N.; Wilkin, Francis P.

The Astronomical Journal, Volume 170, Issue 5, id.287, 34 pp.

We present ExoMiner++, an enhanced deep learning model that builds on the success of ExoMiner to improve transit signal classification in 2-minute TESS data. ExoMiner++ incorporates additional diagnostic inputs, including periodogram, flux trend, difference image, unfolded flux, and spacecraft attitude control data, all of which are crucial for effectively distinguishing transit signals from more challenging sources of false positives (FPs). To further enhance performance, we leverage multisource training by combining high-quality labeled data from the Kepler space telescope with TESS data. This approach mitigates the impact of TESS's noisier and more ambiguous labels. ExoMiner++ achieves high accuracy across various classification and ranking metrics, significantly narrowing the search space for follow-up investigations to confirm new planets. To serve the exoplanet community, we introduce a new TESS catalog containing ExoMiner++ classifications and confidence scores for each transit signal. Among the 147,568 unlabeled TCEs, ExoMiner++ identifies 7330 as planet candidates (PCs), with the remainder classified as FPs. These 7330 PCs correspond to 1868 existing TESS Objects of Interest (TOIs), 69 Community TESS Objects of Interest (CTOIs), and 50 newly introduced CTOIs. 1797 out of the 2506 TOIs previously labeled as PCs in ExoFOP are classified as PCs by ExoMiner++. This reduction in plausible candidates, combined with the excellent ranking quality of ExoMiner++, allows the follow-up efforts to be focused on the most likely candidates, increasing the overall planet yield.

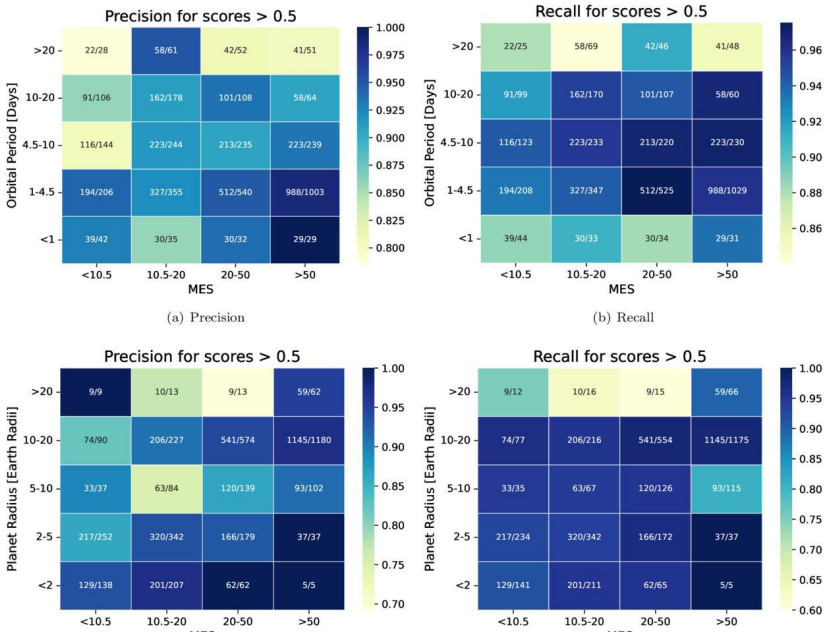

(a) Precision (b) Recall

Figure 15. *Precision and recall heatmaps as functions of MES, orbital period (days), and planet radius (Earth radii).*

HWO Target Stars and Systems: A Prioritized Community List of Potential Stellar Targets for the Habitable Worlds Observatory's ExoEarth Survey

Tuchow, Noah W.; Harada, Caleb K.; Mamajek, Eric E.; Tanner, Angelle; Hinkel, Natalie R.; Belikov, Ruslan; Sirbu, Dan; Ciardi, David R.; Stark, Christopher C. ; Morgan, Rhonda M.; Savransky, Dmitry; Turmon, Michael

Publications of the Astronomical Society of the Pacific, Volume 137, Issue 10, id.104402, 10 pp.

The HWO Target Stars and Systems 2025 (TSS25) list is a community-developed catalog of potential stellar targets for the Habitable Worlds Observatory (HWO) in its survey to directly image Earth-sized planets in the habitable zone. The TSS25 list categorizes potential HWO targets into priority tiers based on their likelihood to be surveyed and the necessity of obtaining observations of their stellar properties prior to the launch of the mission. This target list builds upon previous efforts to identify direct imaging targets and incorporates the results of multiple yield calculations assessing the science return of current design concepts for HWO. The TSS25 list identifies a sample of target stars that have a high probability to be observed by HWO (Tiers 1 and 2), independent of assumptions about the mission's final architecture. These stars should be the focus of community precursor science efforts in order to mitigate risks and maximize the science output of HWO. This target list is publicly available and is a living catalog that will be continually updated leading up to the mission.

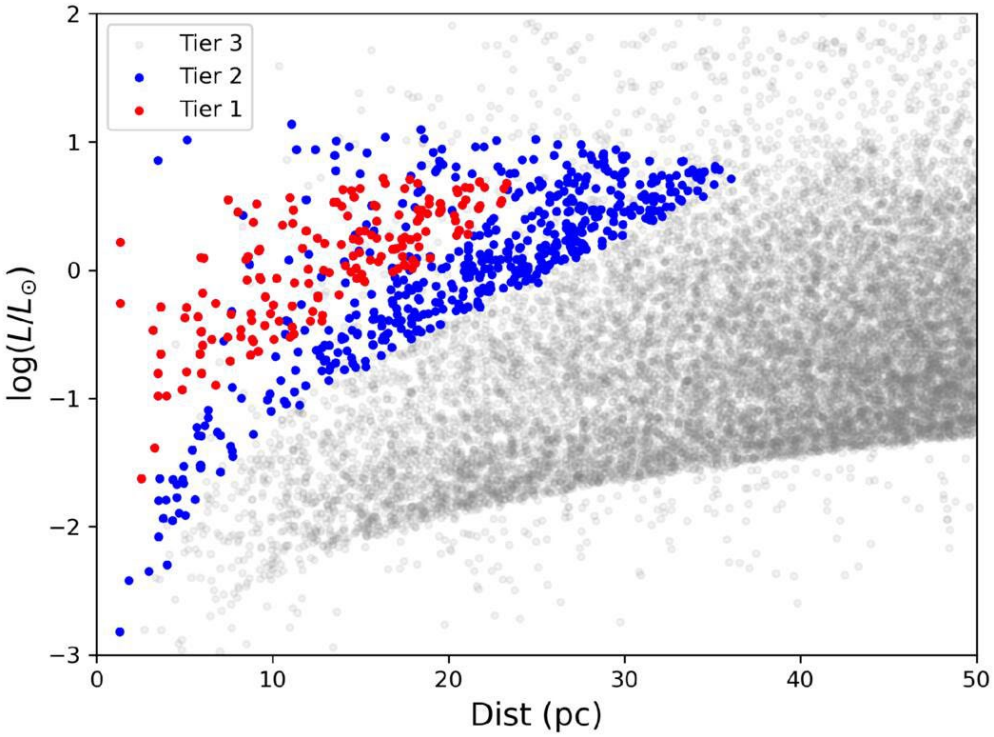

***Figure 3**. Targets in all tiers of our catalog plotted in distance vs. luminosity space, with the tiers indicated by color.*

Diversity in Planetary Architectures from Pebble Accretion: Water Delivery to the Habitable Zone with Pebble Snow

McCloat, Sean search by orcid ; Mulders, Gijs D. search by orcid ; Fieber-Beyer, Sherry

The Astrophysical Journal, Volume 992, Issue 2, id.200, 15 pp.

"Pebble snow" describes a planet formation mechanism where icy pebbles in the outer disk reach inner planet embryos as the water-ice line evolves inward. We model the effects pebble snow has on sculpting planetary system architectures by developing the "PPOLs model." The model is capable of growing any number of protoplanet seed masses by pebble accretion simultaneously, and accounts for differences in rocky and icy pebble composition, the filtering of pebbles by other protoplanets, the pebble isolation mass, and a self-consistently evolving snow line. The growth and bulk composition are recorded across a grid of protoplanetary disks with stellar masses ranging from 0.125 to 2.0 M⊙ (M to A stars) and disk masses ranging from 1% to 40% of the stellar mass. Three system architectures emerge following a low, medium, and high disk mass fraction that remains consistent across stellar mass. The low-mass architecture is the only one to yield short-period Mars- to Earth-mass cores with bulk water content spanning orders of magnitude and may be a prelude to observed "peas in pod" systems. The high-mass architecture produces proto–gas giant cores in the outer disk. The medium-mass architecture produces a bimodal peak in mass within a system, with the outer protoplanet mass at the snow line growing to an order of magnitude larger, resembling the solar system. Solar system–like architectures appear for a small range of initial disk masses around F and G stars, but are not a common feature around K and M stars.

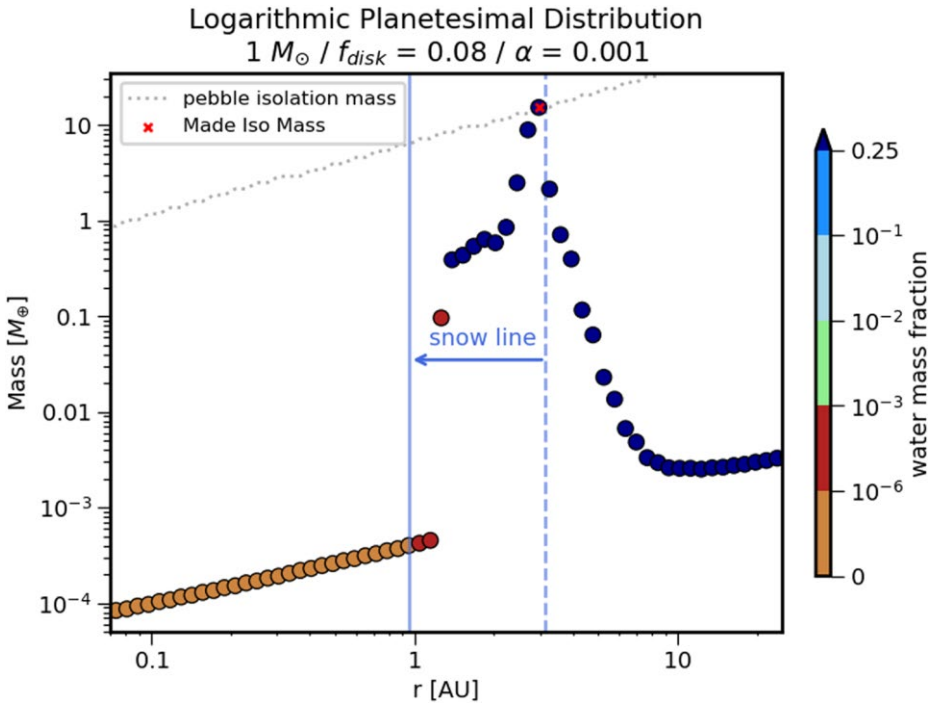

***Figure 9**. Protoplanet masses around a 1 $M_\oplus$ star using a logarithmic distribution of planetesimal seed mass and introduction time, with the same disk parameters as Figure 3, middle panel. The later introduction of outer seeds does not filter the inward pebble flux enough to prevent the seed mass at 3 au from reaching pebble isolation mass (red "×").*

Gravity-sensitive Spectral Indices in Ultracool Dwarfs: Investigating Correlations with Metallicity and Planet Occurrence Using SpeX and Fire Observations

Davoudi, Fatemeh; Rackham, Benjamin V.; de Wit, Julien; Toomlaid, Jan; Gillon, Michaël; Triaud, Amaury H. M. J.; Burgasser, Adam J.; Theissen, Christopher A.

The Astronomical Journal, Volume 170, Issue 4, id.213, 14 pp.

We present a near-infrared spectroscopic analysis (0.9–2.4 μm) of gravity indices for 56 ultracool dwarfs (M5.5–L0), including exoplanet hosts SPECULOOS-2, SPECULOOS-3, and LHS 3154. Our dataset includes 59 spectra from the SpeX and FIRE spectrographs. We also discuss literature results for TRAPPIST-1. Using gravity-sensitive spectral indices, including FeH absorption (0.99, 1.20, and 1.55 μm), the VO band at 1.06 μm, the H-band continuum, and alkali lines such as K I (1.17 and 1.25 μm), we investigate correlations between gravity classification, stellar metallicity, and the presence of close-in transiting planets. All four planet-hosting stars exhibit intermediate-gravity spectral signatures, despite indicators of field age. However, a volume-corrected logistic regression reveals no significant association between gravity class and planet occurrence. Among individual indices, we find FeH_z to be the most promising tracer of planet-hosting status. We tentatively identify a correlation between FeH_z (0.99 μm) and planet presence at the 2σ level, though the result may reflect observational biases, including transit probability, small-number statistics, and detection sensitivity. More robustly, we find a significant anticorrelation between FeH_z and [Fe/H] (3.3σ). A Kruskal–Wallis test shows no significant [Fe/H] difference across gravity classes, suggesting the observed FeH_z–[Fe/H] trend is not driven by bulk metallicity differences. We propose this anticorrelation may reflect the interplay between age, gravity, and composition: higher-metallicity objects may be systematically younger and have lower gravities, suppressing FeH absorption. While our results only hint at a link between gravity-related characteristics and planet occurrence among late-M dwarfs, they underscore the need for caution when using spectral diagnostics to infer the properties of planet-hosting ultracool dwarfs.

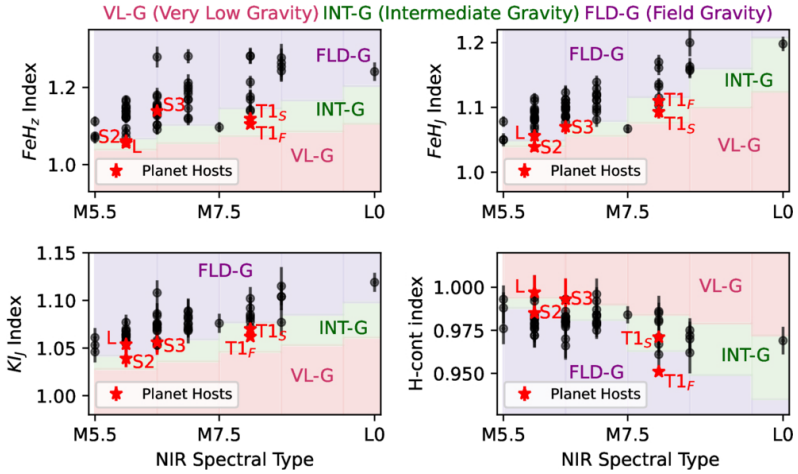

***Figure 3**. Gravity indices (FeH_z, FeH_J, K I_J and H-cont) vs. NIR spectral type for M dwarfs in our sample. The color-coded regions represent different gravity classifications: Very Low Gravity (VL-G, pink), Intermediate Gravity (INT-G, green), and Field Gravity (FLD-G, purple). SPECULOOS-2 (S2), SPECULOOS-3 (S3), LHS 3154 (L), and the FIRE and SpeX spectra measurements of TRAPPIST-1 ($T1_F$ and $T1_S$) are highlighted as red stars.*

PLATOSpec's first results: Planets WASP-35b and TOI-622b are on aligned orbits, and K2-237b is on a polar orbit

Zak, J.; Kabath, P.; Boffin, H. M. J.; Liptak, J. ; Skarka, M.; Brahm, R. ; Gajdoš, P.; Bocchieri, A.; Itrich, D.; Vanzi, L.; Pintr, P. ; Janik, J.; Hatzes, A.

Astronomy & Astrophysics, Volume 702, id.A266, 11 pp.

The spin-orbit angle between a stellar spin axis and its planetary orbital axis is a key diagnostic of planetary migration pathways, yet the mechanisms shaping the observed spin-orbit distribution remain incompletely understood. Combining the spin–orbit angle with atmospheric measurements has emerged as a powerful method of studying exoplanets that showcases the synergy between ground-and space-based observations. We present the Rossiter-McLaughlin effect measurements of the projected spin-orbit angle (λ) for three gaseous exoplanets using the newly commissioned PLATOSpec instrument on the E152 Telescope at La Silla Observatory. For WASP-35b, we determine λ = 1-18+19 deg, demonstrating PLATOSpec's capabilities through excellent agreement with HARPS-N literature data. We provide the first spin-orbit measurements for TOI-622b (λ = -4 ± 12 deg, true spin-orbit angle ψ = 16.1-9.7+8.0 deg), revealing an aligned orbit consistent with quiescent disk migration. For K2-237b, we find λ = 91 ± 7 deg and ψ = 90.5-6.2+6.8 deg, indicating a nearly perfect polar orbit, which suggests a history consistent with disk-free migration, contrasting with previous studies inferring disk migration. TOI-622b populates a sparsely populated region of sub-Jovian planets with measured spin-orbit angles orbiting stars above the Kraft break, while K2-237b's polar configuration strengthens tentative evidence of preferential orbital orientations. All three systems are compelling targets for future atmospheric characterization, and these dynamical constraints will be vital for a comprehensive understanding of their formation and evolution.

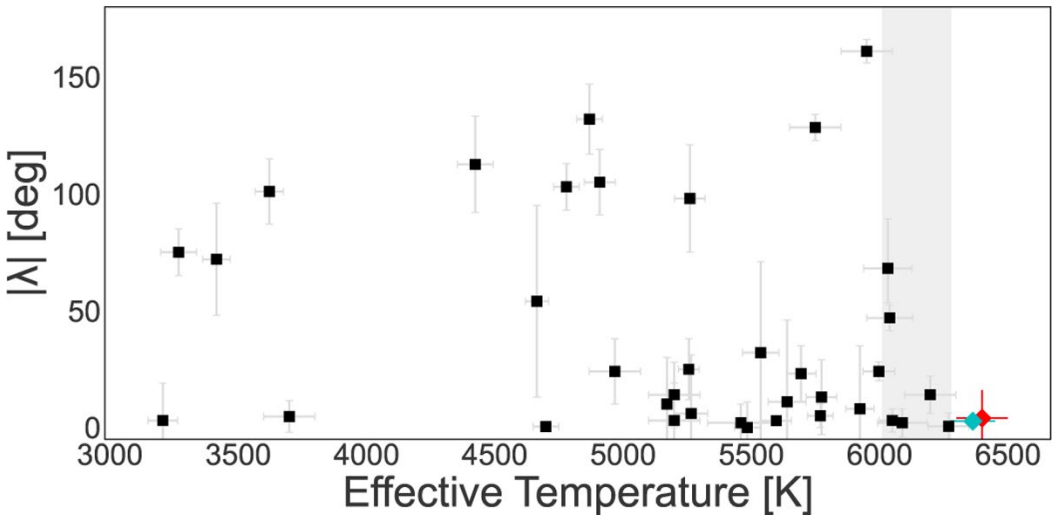

***Figure 5**. Projected spin–orbit angle versus stellar effective temperature for the sub-Jovian population ($M_p \lesssim 0.3\ M_{Jup}$). The gray area shows the position of the Kraft break derived in Spalding & Winn (2022). The literature values were retrieved from the TEPCat catalogue (Southworth 2011). TOI-622b is plotted in red. TOI-622b joins the rare population of sub-Jovian planets around hot stars, and similarly to HD 106315c (cyan), orbits a star located above the Kraft break.*